

PLASMACHEMICAL DOUBLE CLICK THIOL-ENE REACTIONS FOR WET ELECTRICAL BARRIER

R. C. Fraser, A. Carletto, M. Wilson, and J. P. S. Badyal*

Chemistry Department, Science Laboratories, Durham University, Durham DH1 3LE,
England, UK

* Corresponding author email: j.p.badyal@durham.ac.uk

KEYWORDS

Plasmachemical deposition; thiol-ene click reaction; wet electrical barrier; multilayer; electronics.

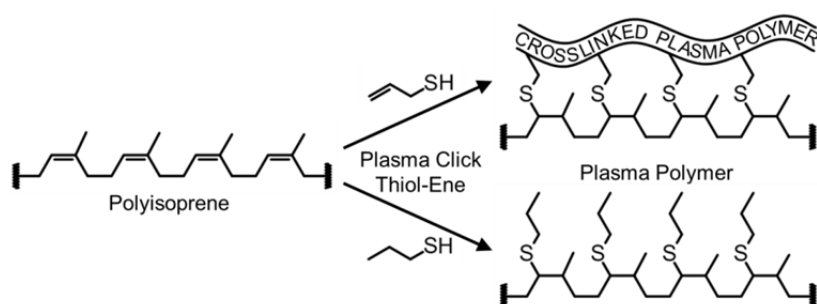
ABSTRACT

Click thiol-ene chemistry is demonstrated for the reaction of thiol containing molecules with surface alkene bonds during electrical discharge activation. This plasmachemical reaction mechanism is shown to be two-fold for allyl mercaptan (an alkene and thiol group containing precursor), comprising self-crosslinked nanolayer deposition in tandem with interfacial crosslinking to the surface alkene bonds of a polyisoprene base layer. A synergistic multilayer structure is attained which displays high wet electrical barrier performance during immersion in water.

1 INTRODUCTION

The continual drive towards smaller portable electronics with greater functionality (e.g. smartphones and wearable devices) is leading to more stringent demands for device performance (e.g. operation during immersion in water or protection against accidental spillage).¹ Hence, there exists a strong demand for high electrical barrier coatings which block water ingress in order to prevent device failure through corrosion, degradation, or electrical short circuiting.² Polymeric layers are at the forefront of such protective coatings due to their high electrical insulation and low permeation properties.^{3,4} Examples include polystyrene,⁵ parylene,⁶ urethane modified polybutadiene,⁷ polymer composites,⁸ amorphous hydrocarbon films,^{9,10} plasma deposited polysilicon coatings,¹¹ and plasma polymers.¹² Further enhancement of electrical barrier properties can be achieved through crosslinking,^{13,14} or multilayering. In the case of the latter, the layering of ultra-thin films helps to block pin-hole defects.^{15,16,17,18} Therefore, in principle, a combination of crosslinking and multilayering should lead to further improvement in electrical barrier performance.¹⁹ However, existing fabrication processes suffer from being long winded, involving multiple lengthy steps as well as requiring elevated temperatures.

In this article, the attributes of combining interfacial crosslinking with multilayering is accomplished through the utilisation of plasmachemical thiol-ene click reactions leading to high wet electrical barrier performance.²⁰ A structure-behaviour relationship study has shown that an alkene-thiol precursor (allyl mercaptan) undergoes the formation of a thiol-ene self-crosslinked nanolayer in tandem with interfacial crosslinking to an alkene bond containing polymer base layer (polyisoprene), Scheme 1.



Scheme 1: Interfacial thiol-ene crosslinked barrier formation between polyisoprene base layer and 1-propanethiol versus allyl mercaptan plasma polymers. The latter undergoes additional thiol-ene crosslinking between adjacent precursor molecule thiol and alkene groups.^{21,22}

2 EXPERIMENTAL

2.1 *Micro-Circuit Board Fabrication*

Single sided copper clad micro-circuit boards were prepared using a photoresist board (manufacturer part code 141300, Kelan Circuits Ltd., comprising epoxy woven glass laminate base (National Electrical Manufacturers Association grade FR4 and British Standard BS4584) coated with a 35 μm copper foil and a photoresist top layer (Photoposit SP24, Dow Chemical Company)). A negative image mask (designed using Easy-PC 2000 (version 19) software, Number One Systems Ltd.) was printed onto 100 μm thickness transparent polymer sheets (product code 0224010460, Ryman UK Ltd.) using black ink (product number PGI-520BK, Canon Inc.) and an inkjet printer (model IP3600, Canon Inc.). This negative image mask was then placed on top of the photoresist board, and exposed to UV irradiation (368 nm, 15 W, 2 min exposure, model LV204, Mega Electronics Inc.), Figure 1. The UV degraded photoresist regions were dissolved off by immersion into a developer solution for 30 s (1.5% w/v NaOH and 1.5% w/v KOH in water, product code AZ303, GSPK Circuits Ltd.) revealing underlying copper, which was then etched away by dipping into 50% w/v ferric chloride solution for 5 min (ferric chloride pellets (product code 3205022, Mega Electronics Inc.) mixed with 40–50 °C tap water (Northumbrian Water), contained in a bubble etch tank, (model PA104, Mega Electronics Inc.)). Next, the photoresist board was rinsed under tap water to wash away any remaining ferric chloride solution. Finally, the unexposed protective photoresist regions were removed by gently rinsing the surface in acetone (+99.8 wt%, Fisher Scientific Ltd.), followed by soaking in propan-2-ol (+99.5 wt%, Fisher Scientific Ltd.) for 20 min.

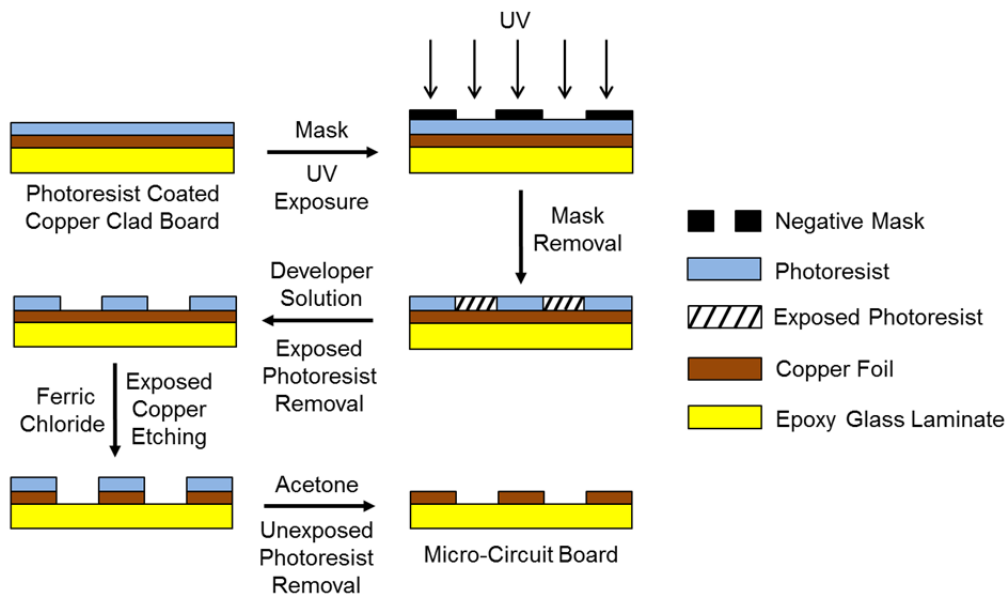


Figure 1: Copper track micro-circuit board fabrication.

The fabricated micro-circuit board layout consisted of two copper contact pads connected to respective copper tracks (separated by 0.8 mm) on top of the epoxy glass laminate substrate, Figure 2. A small strip of single-sided adhesive tape (product code 1443170, Henkel Ltd.) was applied to the contact pads prior to film deposition in order to mask them (i.e. keep them clean for subsequent electrical test connection).

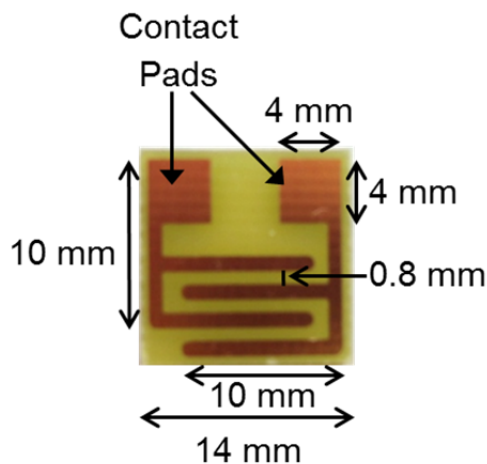


Figure 2: Test micro-circuit board copper tracks separated by a 0.8 mm gap.

2.2 Spin Coating Polymer Base Layer

Following spin coating of polybutadiene, polyisoprene, and polystyrene base layers, the micro-circuit boards were left to dry in a vacuum oven at 60 °C for 60 min in order to remove any trapped solvent (see Supporting Information). Then the underside of each micro-circuit board was carefully cleaned using a cotton bud soaked in acetone, in order to remove any remaining traces of double-sided adhesive tape which had previously been used to hold the micro-circuit board in place during spin coating. Care was taken to ensure that no acetone came into contact with the coated topside. Prior to further testing, the coatings were visually inspected for the absence of defects.

2.3 Plasmachemical Deposition

Plasma treatments were carried out at room temperature in a cylindrical glass reactor (5 cm diameter, 470 cm³ volume) connected to a two stage rotary pump (model E2M2, Edwards Vacuum Ltd.) via a liquid nitrogen cold trap, (base pressure of 4×10^{-3} mbar and an air leak rate better than 1×10^{-9} mol s⁻¹).²³ An L-C matching unit was used to minimize the standing wave ratio (SWR) of the power transmitted from a 13.56 MHz radio frequency (RF) generator to a copper coil (4 mm diameter, 10 turns, spanning 8 cm) externally wound around the glass chamber.²⁴ A signal generator (model TG503, Thurlby Thandar Instruments Ltd.) was used to trigger the RF power supply for the case of pulsed plasma deposition. Prior to each plasma treatment, the chamber was scrubbed with detergent, rinsed with propan-2-ol (+99.5 wt%, Fisher Scientific Ltd.), and further cleaned using a 50 W air plasma for at least 30 min. The precursors used for plasma deposition were 1H,1H,2H,2H-perfluorooctyl acrylate (PFAC-6, +95 wt% purity, Fluorochem Ltd.), glycidyl methacrylate (GMA, +97 wt% purity, Sigma-Aldrich Co.), tetramethylsilane (TMS, +99.9 wt% purity, Alfa Aesar Co. Ltd.), 1-propanethiol (+99 wt% purity, Sigma-Aldrich Co.), and allyl mercaptan (2-propene-1-thiol, +80 wt% purity, Tokyo Chemical Industry Ltd.). The precursors were degassed prior to use by 5 freeze-pump-thaw cycles. Control plasma surface modification using hydrogen sulfide (+99.5% purity, Aldrich Chemical Co.) was also carried out. For each case, polymer base layer coated micro-circuit boards were placed into the centre of the plasma reactor followed by evacuation to

system base pressure. 0.2 mbar of precursor vapour was then introduced into the chamber via a fine control needle valve (model LV10K, Edwards Vacuum Ltd.) at a flow rate of $1.7 \times 10^{-7} \text{ mol s}^{-1}$, and the reactor was purged for 5 min, followed by ignition of the electrical discharge. Film deposition / surface modification was allowed to proceed for a predetermined period, and then the power supply was switched off whilst maintaining precursor flow through the reactor for a further 5 min in order to quench any reactive surface sites before evacuation to base pressure.

2.4 Film Thickness

Film thickness measurements were carried out on coated silicon pieces (1 cm^2 , 5–20 $\Omega \text{ cm}^{-1}$ resistivity, Silicon Valley Microelectronics Inc.) using a spectrophotometer (model nkd-6000, Aquila Instruments Ltd.). The obtained transmittance-reflectance curves (350–1000 nm wavelength range and parallel (P) polarised light source at a 30° incident angle) were fitted to a Cauchy model for dielectric materials,²⁵ using a modified Levenberg-Marquardt method (version 2.2 software, Pro-Optix, Aquila Instruments Ltd.).²⁶ The coated micro-circuit boards lacked sufficient reflectivity for thickness measurements using this technique, and therefore silicon wafer pieces were used instead by placing them alongside the micro-circuit boards during plasma deposition.

2.5 Wet Electrical Barrier Measurement

The immersion in water of coated micro-circuit boards whilst measuring electrical resistance is a realistic test for evaluating electrical barrier performance.²⁷ Tap water ($156 \mu\text{S cm}^{-1}$ conductivity, Northumbrian Water), representing a “real world” scenario for water damage to consumer electronics, was allowed to equilibrate to room temperature (20°C) prior to usage. A multimeter (with a lower detection limit of 10 nA, Keithley 2000, Tektronix UK Ltd.) was used to measure the current flow for each coated micro-circuit board connected to a variable voltage supply (Model PS-6010, Instek Ltd.), Figure 3. The voltage applied across the circuit was checked using a handheld multimeter (model 72-770, TENMA Ltd.). Standard wires and connectors

were employed (Flexiplast 2V, stranded wire, 0.75 mm² cross sectional area, 129 strands, 0.07 mm diameter, negligible internal resistance, Multi-Contact UK Ltd.).

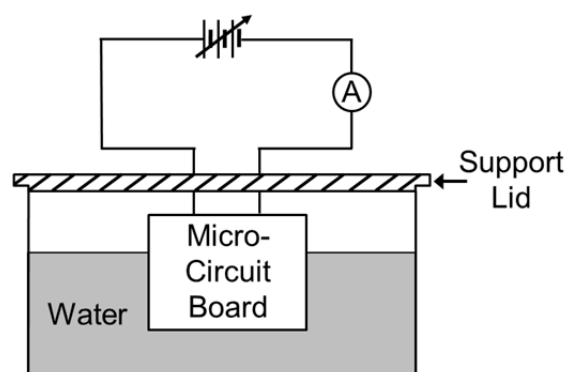


Figure 3: Circuit diagram for wet electrical barrier testing. See Supporting Information Figure S 1 for further details.

Two small crocodile clips were carefully cleaned with acetone in order to remove any contaminants, and then fed through two holes in a support lid used to hold the micro-circuit board in place, Supporting Information Figure S 1. This was lowered into a 50 mL glass jar filled with 32.5 mL of equilibrated tap water.

A fixed voltage was then applied across the 0.8 mm gap between the micro-circuit board copper tracks whilst immersed in water (e.g. 8 V corresponds to an electric field of 10 V mm⁻¹). Current measurements were taken every 30 s over a 13 min period.²⁸ At this stage, the final electrical resistance was calculated using Ohm's law. This resistance value was then divided by the total coating thickness (plasma polymer and polymer base layer combined) in order to yield the electrical barrier performance (units $\Omega \text{ nm}^{-1}$).

2.6 X-Ray Photoelectron Spectroscopy

X-ray photoelectron spectroscopy (XPS) analysis of the plasma deposited 1-propanethiol and allyl mercaptan layers was carried out using a VG ESCALAB II electron spectrometer equipped with a non-monochromated Mg K α X-ray source (1253.6 eV) and a concentric hemispherical analyser. Photoemitted electrons were collected at a take-off angle of 20° from the substrate normal, with electron detection in the constant analyser energy mode (CAE, pass energy = 20 eV and 50 eV for high

resolution and survey scans respectively). Instrument sensitivity (multiplication) factors were experimentally determined to be C(1s):S(2p):O(1s) equals 1.00:0.57:0.35 by using a polysulfone standard (0.005 in film, Westlake Plastics Company Inc.).^{29,30} All binding energies were referenced to the C(1s) hydrocarbon peak at 285.0 eV.²⁹ A linear background was subtracted from each core level spectrum and then fitted using fixed full width half maximum (FWHM) Gaussian peaks.³¹

2.7 Infrared Spectroscopy

Fourier transform infrared (FTIR) analysis of the 1-propanethiol and allyl mercaptan precursors was performed using a FTIR spectrometer (Spectrum Two, PerkinElmer Inc.) fitted with a transmission cell and a deuterated triglycine sulfate (DTGS) detector. Spectra were acquired across the 450–4000 cm^{-1} range and averaged over 16 scans at a resolution of 4 cm^{-1} . A droplet of precursor was dispensed between two KBr plates and spectra taken. Reflection-absorption infrared spectroscopy (RAIRS) analysis of plasma deposited layers onto silicon wafers (Silicon Valley Microelectronics, Inc.) was carried out using a liquid nitrogen cooled mercury cadmium telluride (MCT) detector (Spectrum One, PerkinElmer Inc.) and a variable angle accessory (Specac Ltd.) fitted with mirrors aligned at an angle of 66° to the sample normal. The spectra were averaged over 285 scans at a resolution of 4 cm^{-1} .

3 RESULTS AND DISCUSSION

3.1 Plasma Deposited Top Layer

Diffusion of aqueous ions through a barrier layer towards an underlying electronic circuit governs the overall level of device protection, and therefore electrical resistance measurements taken during water immersion are a strong indicator of a coating's wet electrical barrier performance.^{32,33} A structure-behaviour relationship study screened precursors containing a range of different functional groups for

plasma deposition onto a polybutadiene base layer: 1H,1H,2H,2H-perfluorooctyl acrylate, glycidyl methacrylate, tetramethylsilane, 1-propanethiol, and allyl mercaptan, Figure 4. A general trend was found showing an improvement in wet electrical barrier with increasing plasma polymer layer thickness; for instance in the case of both glycidyl methacrylate and tetramethylsilane precursors, an absence of current flow was reached for thicknesses exceeding 1.4 μm . The thinnest plasma deposited layers displaying high electrical barrier were obtained for allyl mercaptan precursor; whilst in contrast, structurally related 1-propanethiol (which contains no carbon-carbon double bond) was found to be poor at comparable thicknesses, Figure 4 and Figure 5. It is evident that the plasma deposited allyl mercaptan layer does not follow the general trend observed for the other precursors screened (the latter show increased layer thickness leads to a gradual improvement in wet electrical barrier). H_2S plasma modification of polybutadiene was employed as a control to verify that surface sulfonation alone is insufficient to attain good wet electrical barrier performance. The high wet electrical barrier measured for allyl mercaptan plasma polymer coating exceeds the performance found for existing coatings, such as 1H,1H,2H,2H-perfluorooctyl acrylate plasma polymer, Figure 4.³⁴

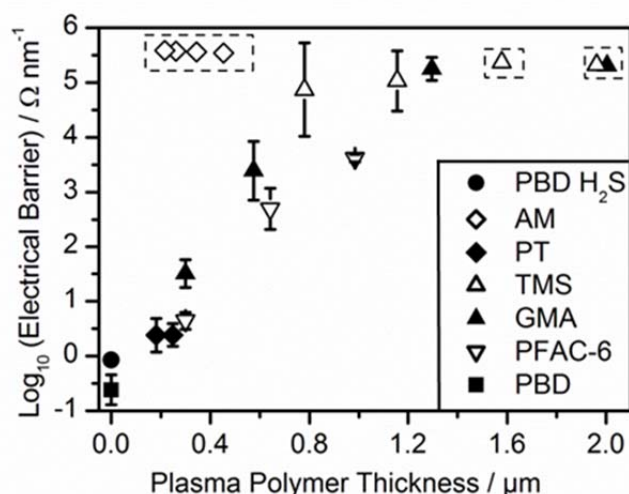


Figure 4: Wet electrical barrier after 13 min immersion in water under an applied electric field of 10 V mm^{-1} , for a range of plasma polymers deposited onto spin coated polybutadiene base layer (thickness $1872 \pm 39 \text{ nm}$): 1H,1H,2H,2H-perfluorooctyl acrylate (PFAC-6, pulsed duty cycle $t_{on} = 20 \mu\text{s}$, $t_{off} = 20 \text{ ms}$, and $P_{on} = 40 \text{ W}$); glycidyl methacrylate (GMA, continuous wave 5 W); tetramethylsilane (TMS, continuous wave 3 W); 1-propanethiol (PT, continuous wave 2 W); and allyl mercaptan (AM, continuous wave 2 W) precursors. Polybutadiene base layer (PBD) and following H_2S plasma exposure (PBD hydrogen sulfide, continuous wave 2

W) are included as controls. Samples marked within dashed boxes reached the instrument detection limit of $8 \times 10^8 \Omega$. Wet electrical barrier values measured at the beginning of water immersion ($t = 0$ min) are reported in Supporting Information Table S 1.

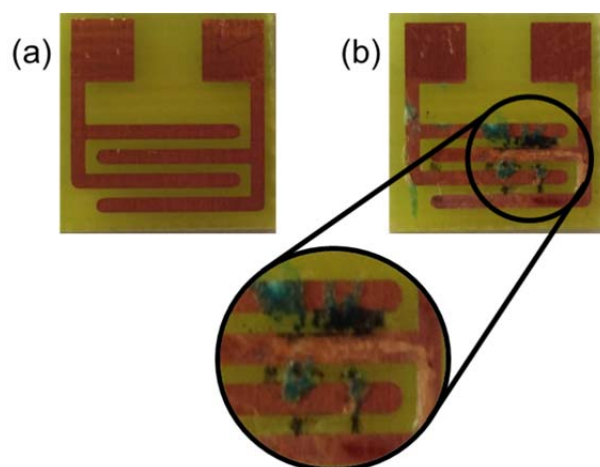


Figure 5: Micro-circuit board photographs taken after wet electrical barrier testing (10 V mm^{-1} electric field applied for 13 min): (a) allyl mercaptan plasma polymer on polyisoprene base layer; and (b) 1-propanethiol plasma polymer on polyisoprene base layer. The plasma polymer thickness was $555 \pm 23 \text{ nm}$, and the polyisoprene base layer thickness was $1353 \pm 40 \text{ nm}$. Similar results were obtained when a polybutadiene base layer was used instead of polyisoprene.

No correlation was found between wet electrical barrier and static water contact angle values, Figure 4 and Supporting Information Table S 2. The most hydrophobic plasma deposited coating (1H,1H,2H,2H-perfluorooctyl acrylate) showed a relatively poor wet electrical barrier performance, whilst the best performing coating (allyl mercaptan) had a comparatively low water contact angle.

For both 1-propanethiol and allyl mercaptan plasma polymers, XPS analysis detected the presence of elemental carbon, sulfur, and a small amount of oxygen, Table 1 and Supporting Information Figure S 2. The low level of oxygen can be attributed to some aerial surface oxidation during sample transfer from the plasma deposition chamber.^{35,36} The C(1s) spectra were consistent with hydrocarbon (285.0 eV) and carbon-sulfur (286.9 eV) environments, Supporting Information Figure S 2.²⁹ No significant difference in the measured sulfur concentration was found between the 1-propanethiol and allyl mercaptan plasma polymer layers. The S(2p_{3/2}) and S(2p_{1/2}) component peak binding energies are consistent with C-S-C^{29,30} or C-S-H (thiol) environments,^{37,38,39} and do not correspond to oxidised sulfur (S(2p_{3/2}) binding energy range 166–168 eV).^{29,37}

Table 1: Elemental XPS compositions for 1-propanethiol and allyl mercaptan plasma polymer layers (continuous wave 2 W).

| Sample | C(1s) | | S(2p) | | | O(1s) | |
|--------------------------------|--------|----------------|--------|---------------------------------|---------------------------------|-------|-------------------|
| | % | Main Peak / eV | % | S(2p _{3/2}) Peak / eV | S(2p _{1/2}) Peak / eV | % | Peak Maximum / eV |
| 1-Propanethiol Theoretical | 75 | - | 25 | - | - | 0 | - |
| 1-Propanethiol Plasma Polymer | 65 ± 1 | 285.0 | 32 ± 2 | 164.0 | 165.2 | 3 ± 2 | 532.2 |
| Allyl Mercaptan Theoretical | 75 | - | 25 | - | - | 0 | - |
| Allyl Mercaptan Plasma Polymer | 62 ± 1 | 285.0 | 35 ± 3 | 163.6 | 164.8 | 3 ± 2 | 531.7 |

The infrared spectrum of allyl mercaptan precursor displays a strong allyl CH₂ stretch absorbance (3080 cm⁻¹),⁴⁰ which disappears upon plasma deposition, Figure 6. As expected, this feature was absent for both 1-propanethiol monomer and its corresponding plasma polymer. Both 1-propanethiol and allyl mercaptan precursors show a weak S-H stretch (2555 cm⁻¹),^{40,41} which is also observed for plasma deposited allyl mercaptan; however it was absent for plasma deposited 1-propanethiol.

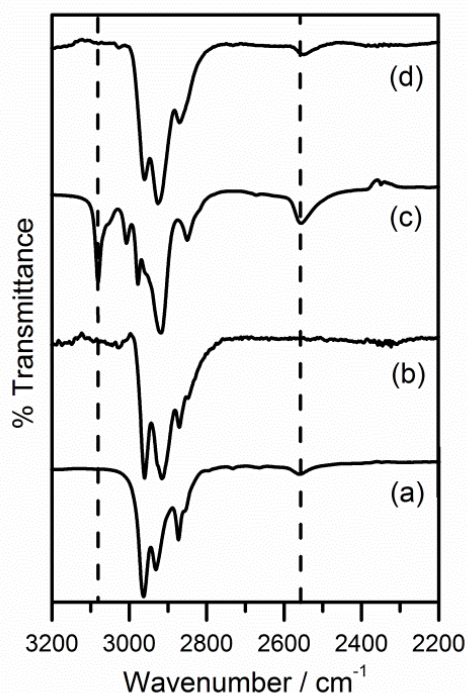


Figure 6: FTIR infrared spectra of: (a) liquid 1-propanethiol; (b) continuous wave 2 W plasma deposited 1-propanethiol; (c) liquid allyl mercaptan; and (d) continuous wave 2 W plasma deposited allyl mercaptan. Dashed lines indicate allyl CH₂ (3080 cm⁻¹) and thiol S-H (2555 cm⁻¹) stretches respectively.

Several orders of magnitude improvement in wet electrical barrier performance has been found following allyl mercaptan plasma polymer deposition onto a polybutadiene base layer ($> 10^5 \Omega \text{ nm}^{-1}$), Figure 4. Furthermore, despite the similar chemical structures of allyl mercaptan and 1-propanethiol precursor molecules, their corresponding plasma deposited films display markedly different wet electrical barrier performances. This may be attributed to the allyl mercaptan carbon-carbon double bond playing a key role, Scheme 1. Two complementary sets of thiol-ene click chemistry crosslinking reactions are envisaged^{20,42,43}: firstly there is the plasma deposited layer thiol groups reacting with carbon-carbon alkene bonds present within the underlying polymer base layer (e.g. polybutadiene); and secondly the allyl mercaptan thiol groups can crosslink and self-polymerise with adjacent monomer carbon-carbon double bonds during plasmachemical deposition, Scheme 1.^{21,44} In both cases, the prerequisite thiyl radicals required for thiol-ene click chemistry are generated in-situ by the electrical discharge excited species (photons, electrons, etc.) rather than conventional thermal or photochemical initiation.^{45,46} Such sulfur

crosslinking improves hardness, strength, and durability of bulk polymers.^{47,48,49} Overall, this gives rise to an allyl mercaptan plasma deposited sulfur crosslinked top layer which is also sulfur crosslinked to the polybutadiene base layer, leading to a tightly bonded interfacial region for optimal wet electrical barrier performance (synergistic effect). In contrast, thiol-ene click chemistry occurs for 1-propanethiol through its thiol group crosslinking to the polymer base layer alkene bonds, whilst the molecule lacks the polymerisable allyl mercaptan carbon-carbon double bond needed to form a highly crosslinked top layer, hence explaining its relatively poor wet electrical barrier performance, Figure 4 and Scheme 1. Another contributing factor might be the much lower shrinkage stress for allyl sulfide versus propyl sulfide thiol-ene crosslinking.⁵⁰

3.2 Polymer Base Layer

The specific role of the polymer base layer was investigated next by measuring the wet electrical barrier performance of allyl mercaptan plasma layers deposited onto polybutadiene, polyisoprene, and polystyrene, Figure 7. All of these polymers contain unsaturated carbon-carbon bonds, however only the former two contain alkene bonds necessary for thiol-ene reactions with plasma generated reactive sulfur species (e.g. thiyl radicals). Despite the polystyrene base layer exhibiting the highest wet electrical barrier in the absence of a plasma polymer overlayer, no significant improvement was observed following allyl mercaptan plasma polymer deposition. Whereas, in the case of polybutadiene, the electrical barrier showed a marked enhancement with increasing plasma polymer thickness. Polyisoprene was found to be the best performing polymer base layer, with the wet electrical barrier rising sharply beyond 100 nm plasma polymer layer thicknesses to reach an absence of current flow above 300 nm. The role of base layer thickness was further investigated for polyisoprene whilst maintaining a fixed layer thickness of plasma deposited allyl mercaptan, Figure 8. This indicated a significant improvement in wet electrical barrier beyond 500 nm polyisoprene thickness, to reach high electrical barrier performance at approximately 900 nm.

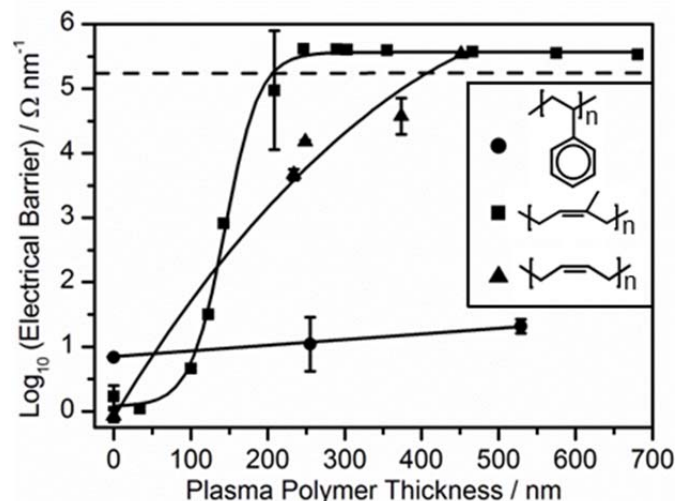


Figure 7: Wet electrical barrier after 13 min immersion in water under an applied electric field of 10 V mm^{-1} , for variable thickness plasma deposited allyl mercaptan (continuous wave 2 W) onto a range of fixed thickness spin coated polymer base layers: polybutadiene (\blacktriangle thickness $1872 \pm 39 \text{ nm}$); polyisoprene (\blacksquare thickness $1681 \pm 35 \text{ nm}$); and polystyrene (\bullet thickness $2037 \pm 195 \text{ nm}$). Samples above the dashed line reached the instrument detection limit of $8 \times 10^8 \Omega$.

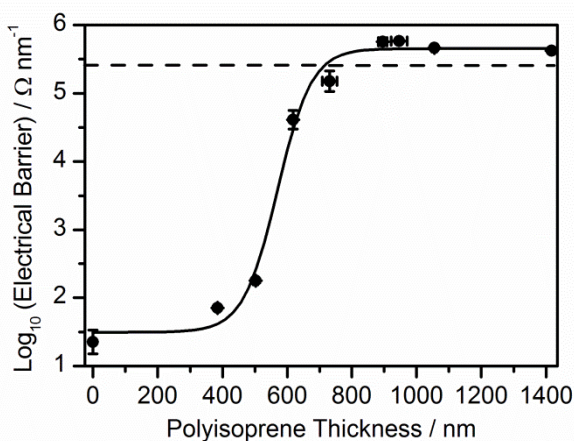


Figure 8: Wet electrical barrier after 13 min immersion in water under an applied electric field of 10 V mm^{-1} , for fixed thickness allyl mercaptan plasma polymer coatings (continuous wave 2 W, $613 \pm 71 \text{ nm}$) deposited onto varying thickness polyisoprene base layers. Samples above the dashed line reached the instrument detection limit of $8 \times 10^8 \Omega$.

For the polymer base layers investigated, comparison of the obtained wet electrical barrier values with standard bulk polymer resistivity values shows that despite polystyrene possessing a high bulk resistivity value, ($> 1 \times 10^{16} \Omega \text{ cm}$),⁵¹ its measured wet electrical barrier value is poor, as was also observed for polyisoprene and polybutadiene, Figure 7. This is most likely due to the relatively high water vapour transmission rates (the mass of water moving through a specified coating area, over a predetermined length of time, normalised to the coating thickness) of

polystyrene (1.60–3.37 g mm m⁻² day⁻¹),⁵² polybutadiene (17.7 g mm m⁻² day⁻¹),⁵³ and vulcanised (crosslinked) polyisoprene (2.4 g mm m⁻² day⁻¹).⁵⁴ Therefore, conventional bulk electrical resistivity values measured in the absence of water cannot be taken as an indication of how well a polymer coating will perform as a wet electrical barrier.

Polybutadiene^{55,56} and polyisoprene^{57,58} have both been reported to undergo conventional thiol-ene click chemistry. Given that thiol-ene click reactions are reported to proceed much faster with electron rich double bonds compared to electron deficient double bonds,^{20,21,59} then one possible explanation for the disparity in wet electrical barrier performance between allyl mercaptan plasma polymer coated polybutadiene versus polyisoprene could be that polyisoprene (which contains an electron donating methyl substituent adjacent to its carbon-carbon double bond),⁶⁰ should display a higher reactivity.⁶¹ The more gradual slope observed for polybutadiene compared to polyisoprene with increasing allyl mercaptan plasma polymer thickness suggests that there is a lower level of interfacial plasmachemical click thiol-ene crosslinking occurring, and therefore thicker films are necessary to achieve sufficient physical barrier for high wet electrical resistance, Figure 4 and Figure 7. Whilst the comparatively poor performance for polystyrene can be attributed to there being a total absence of alkene groups required for thiol-ene click chemistry within the polymer repeat unit.^{62,63}

3.3 Wet Electrical Barrier Breakdown

The wet electrical barrier performance of the optimised thickness allyl mercaptan plasma polymer and polyisoprene layers was then investigated in relation to the magnitude of the applied electric field strength. This showed that the multilayer barrier was stable and resilient up to an applied electric field of 20 V mm⁻¹, beyond which there was some indication of deterioration, Figure 9. Even then, the drop in performance was not severe, with a final wet electrical barrier of 2 x 10⁴ Ω nm⁻¹ being measured at an applied field of 27.5 V mm⁻¹. Compared to modern smartphones, with cell voltages ranging from 3.70–3.85 V,^{64,65} the much higher voltages (up to 20 V) utilised in the present study during wet electrical barrier measurements demonstrate a very good level of performance.

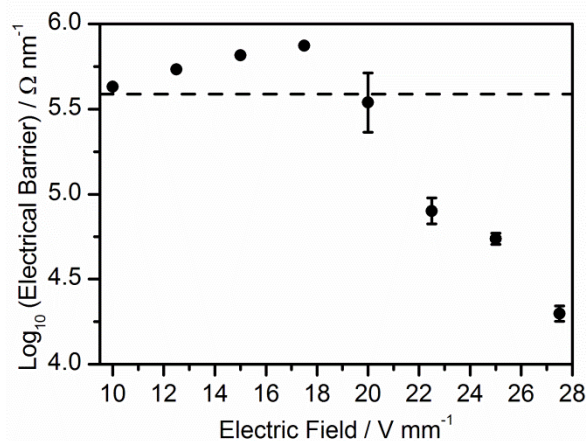


Figure 9: Wet electrical barrier after 13 min immersion in water as a function of applied electric field, for fixed thickness allyl mercaptan plasma polymer (continuous wave 2 W, 507 ± 14 nm) and polyisoprene base layer (1353 ± 40 nm). Samples above the dashed line reached the instrument detection limit.

3.4 Scalability

The described low temperature two step fabrication method for achieving high wet electrical barrier coatings is easily scalable and suitable for high throughput electronic device assembly lines. In the case of non-planar circuit boards (e.g. wearable devices) the polyisoprene base layer can be applied by either spray or dip coating prior to conformal plasma deposition of allyl mercaptan. Future scope for the utilisation of plasmachemical click thiol-ene chemistry could include mixing of allyl thiol or multiple thiol group molecules into alkene bond containing monomer feeds for plasma deposition leading to even greater levels of crosslinking (durability). Alkyne functionalised base layers and alkyne thiols are also potential candidates for plasmachemical thiol-ene click reactions.^{66,67} Other variants include pulsed, downstream, and atmospheric plasmas for generation of the prerequisite thiyl radicals. Additional improvements in wet electrical barrier performance are envisaged by depositing a hydrophobic layer on top of the aforementioned multilayer structure in order to incorporate enhanced liquid repellency, Supporting Information Table S 2.^{68,69,70}

4 CONCLUSIONS

Thiol containing precursors have been found to undergo plasmachemical click thiol-ene reactions with surface alkene bonds. Structure-behaviour relationships have shown that plasmachemical deposition of allyl mercaptan onto a polyisoprene base layer provides a very high level of wet electrical barrier performance. This stems from the allyl mercaptan thiol group undergoing two-fold click thiol-ene reactions with both carbon-carbon alkene bonds contained within adjacent precursor molecules and the underlying polymer base layer, to form an overall tightly bonded multilayer for wet electrical barrier. In contrast, structurally related 1-propanethiol precursor is significantly inferior due to its lack of any carbon-carbon alkene bonds required for click thiol-ene crosslinking within the plasma deposited layer.

5 ACKNOWLEDGEMENTS

R. C. F. and A. C. are grateful to P2i Ltd. for PhD studentships. D. Evans and E. Siokou are thanked for helpful discussions.

6 REFERENCES

- (1) Chen, T.-N.; Wu, D.-S.; Wu, C.-C.; Horng, R.-H.; Wei, H.-F.; Jiang, L.-Y.; Lee, H.-U.; Chang, Y.-Y. Deposition and Characterization of Ultra-High Barrier Coatings for Flexible Electronic Applications. *Vacuum* **2010**, *84*, 1444–1447.
- (2) Hamouda, H. Cathodic Protection. In *Handbook of Environmental Degradation of Materials*; Kutz, M., Ed.; William Andrew Inc.: Norwich, 2005; pp 368–369.
- (3) Kao, K. C. Electrical conduction and breakdown in insulating polymers. In *Properties and Applications of Dielectric Materials*, Proceedings of the 6th International Conference, Xi'an, China, June 21–26, 2000; IEEE Dielectrics and Electrical Insulation Society: New York, 2000, 1–17.
- (4) Goosey, M. T. Permeability Effects in Electrical and Electronic Component Coatings. In *Polymer Permeability*; Comyn, J., Ed.; Elsevier Applied Science Publishers: Essex, 1985; pp 331.
- (5) Lachish, U.; Steinberger, I. T. Electrical Current Measurements on Polystyrene Films. *J. Phys. D: Appl. Phys.* **1974**, *7*, 58–68.
- (6) Charlson, E. J.; Charlson, E. M.; Sharma, A. K.; Yasuda, H. K. Electrical Properties of Glow Discharge Polymers, Parylenes and Composite Films. *J. Appl. Polym. Sci.: Appl. Polym. Symp.* **1984**, *38*, 137–148.
- (7) Battisti, A.; Hirayama, K.; Okuno, A. Unique Polybutadiene Resin: Characteristics After Hardening and Application to IC. In *Electronic Components and Technology Conference*, Proceedings of the 40th Conference, Las Vegas, USA, May 20–23, 1990; IEEE Components Packaging and Manufacturing Technology Society: New York, 1990, 620–624.
- (8) Weng, C.-J.; Chen, Y.-L.; Jhuo, Y. S.; Yi-Li, L.; Yeh, J. M. Advanced Antistatic/Anticorrosion Coatings Prepared from Polystyrene Composites Incorporating Dodecylbenzene Sulfonic Acid-Doped SiO₂ @Polyaniline Core-Shell Microspheres. *Polym. Int.* **2013**, *62*, 774–782.
- (9) Bubenzer, A.; Dischler, B.; Brandt, G.; Koidl, P. Rf-Plasma Deposited Amorphous Hydrogenated Hard Carbon Thin Films: Preparation, Properties and Applications. *J. Appl. Phys.* **1983**, *54*, 4590–4595.
- (10) Biederman, H.; Slavínská, D. Plasma Polymer Films and Their Future Prospects. *Surf. Coat. Technol.* **2000**, *125*, 371–376.

- (11) Lee, J. K.; Cathey, D. A.; Tjaden, K. Method for Forming High Resistance Resistors for Limiting Cathode Current in Field Emission Displays. *Patent* WO1997004482, February 6, 1997.
- (12) Yasuda, H. *Plasma Polymerization*. Academic Press Inc.; Orlando: 1985, pp 395–396.
- (13) Pathak, S. S.; Khanna, A. S.; Sinha, T. J. M. HMMM Cured Corrosion Resistance Waterborne Ormosil Coating for Aluminum Alloy. *Prog. Org. Coat.* **2007**, *60*, 211–218.
- (14) Zandi-Zand, R.; Ershad-Langroudi, A.; Rahimi, A. Silica Based Organic-Inorganic Hybrid Nanocomposite Coatings for Corrosion Protection. *Prog. Org. Coat.* **2005**, *57*, 286–291.
- (15) Batey, J.; Boland, J. J.; Parsons, G. N. Pulsed Gas Plasma-Enhanced Chemical Vapour Deposition of Silicon. *Patent* US5242530, February 7, 1993.
- (16) Yoshida, S.; Okawara, C.; Ozeki, K. Process for Producing Multi-Layered Gas Barrier Film. *Patent* EP2397574, December 21, 2011.
- (17) Graff, G. L.; Williford, R. E.; Burrows, P. E. Mechanisms of Vapour Permeation Through Multilayer Barrier Films: Lag Time Versus Equilibrium Permeation. *J. Appl. Phys.* **2004**, *96*, 1840–1849.
- (18) Graff, G. L.; Gross, M. E.; Affinito, J. D.; Shi, M.-K.; Hall, M. G.; Mast, E. S. Environmental Barrier for Organic Light Emitting Device and Method of Making. *Patent* WO2000036665, June 22, 2000.
- (19) Yamanouchi, S.; Kondo, M.; Inoue, Y. Cross Linked Polyethylene-Insulated Cable. *Patent* EP0111393, June 20, 1984.
- (20) Hoyle, C. E.; Bowman, C. N. Thiol-ene Click Chemistry. *Angew. Chem. Int. Ed.* **2010**, *49*, 1540–1573.
- (21) Jacobine, A. F. Thiol-ene Photopolymers. In *Radiation Curing in Polymer Science and Technology*. Fouassier, J. P.; Rabek, J. F. Eds.; Elsevier Science: Essex; 1993, Vol. 3; pp 247–248.
- (22) Oswald, A. A.; Griesbaum, K. Radical Additions of Thiols to Diolefins and Acetylenes. In *The Chemistry of Organic Sulfur Compounds*. Kharasch, N.; Meyers, C. Y. Eds.; Pergamon Press: Oxford; 1966, Vol. 2; p 238–239.
- (23) Ehrlich, C. D.; Basford, J. A. Recommended Practices for the Calibration and use of Leaks. *J. Vac. Sci. Technol. A* **1992**, *10*, 1–17.
- (24) Hynes, A. M.; Shenton, M. J.; Badyal, J. P. S. Pulsed Plasma Polymerization of Perfluorocyclohexane. *Macromolecules* **1996**, *29*, 4220–4225.

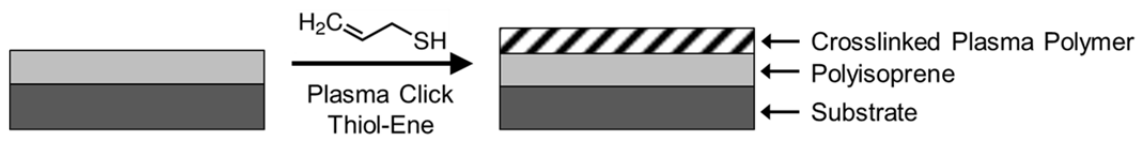
- (25) Diebold, A. C.; Chism, W. W. Characterisation and Metrology of Medium Dielectric Constant Gate Dielectric Films. In *High Dielectric Constant Materials: VLSI MOSFET Applications*; Huff, H. R.; Gilmer, D. C., Eds. Springer-Verlag, Berlin Heidelberg 2005, p 486.
- (26) Lovering, D. NKD-6000 Technical Manual; Aquila Instruments: Cambridge, U.K., 1999.
- (27) International Standard. Degrees of Protection Provided by Enclosures. IEC 60529; Edition 2.1, Section 14.2.7–14.2.8.
- (28) Gupta, V.; Diwan, A.; Evans, D.; Telford, C.; Linford, M. R. Self-Termination in the Gas-Phase Layer-by-Layer Growth of an Aza Silane and Water on Planar Silicon and Nylon Substrates. *J. Vac. Sci. Technol. B* **2014**, *32*, 061803-1–061803-9.
- (29) Moulder, J. F.; Stickle, W. F.; Sobol, P. E.; Bomben, K. D. *Handbook of X-ray Photoelectron Spectroscopy*, Chastain, J., Ed.; Perkin-Elmer Corporation: Eden Prairie, 1992; pp 11–28.
- (30) Beamson, G.; Briggs, D. *High Resolution XPS of Organic Polymers – The Scienta ESCA300 Database*, John Wiley & Sons: Chichester, 1992; pp 258–259.
- (31) Friedman, R. M.; Hudis, J.; Perlman, M. L. Chemical Effects on Linewidths Observed in Photoelectron Spectroscopy. *Phys. Rev. Lett.* **1972**, *29*, 692–695.
- (32) Taylor, S. R. Assessing the Moisture Barrier Properties of Polymeric Coatings Using Electrical and Electrochemical Methods. *IEEE Trans. Electr. Insul.* **1989**, *24*, 787–806
- (33) Sangaj, N. S.; Malshe, V. C. Permeability of Polymers in Protective Organic Coatings – a Review. *Prog. Org. Coat.* **2004**, *50*, 28–39.
- (34) Coulson, S. Novel Products. *Patent* WO 2007/083122, July 26, 2007.
- (35) Donev, S.; Brack, N.; Paris, N. J.; Pigram, P. J.; Singh, N. K.; Usher, B. F. Surface Reactions of 1-Propanethiol on GaAs(100). *Langmuir* **2005**, *21*, 1866–1874.
- (36) Jiang, H.; Grant, J. T.; Enlow, J.; Su, W.; Bunning, T. J. Surface Oxygen in Plasma Polymerized Films. *J. Mater. Chem.* **2009**, *19*, 2234–2239.
- (37) Castner, D. G.; Hinds, K.; Grainger, D. W. X-ray Photoelectron Spectroscopy Sulfur 2p Study of Organic Thiol and Disulfide Binding Interactions with Gold Surfaces. *Langmuir* **1996**, *12*, 5083–5086.
- (38) Roh, J. H.; Lee, J. H.; Kim, N. I.; Kang, H. M.; Yoon, T. -H.; Song, K. H. DSC Analysis of Epoxy Molding Compound with Plasma Polymer-Coated Silica Fillers. *J. Appl. Polym. Sci.* **2003**, *90*, 2508–2516.

- (39) Nuzzo, R. G.; Zegarski, B. R.; Dubois, L. H. Fundamental Studies of the Chemisorption of Organosulfur Compounds on Au(111). Implications for Molecular Self-Assembly on Gold Surfaces. *J. Am. Chem. Soc.* **1987**, *109*, 733–740.
- (40) Lin-Vien, D.; Colthup, N. B.; Fateley, W. G.; Grasselli, J. G. *The Handbook of Infrared and Raman Characteristic Frequencies of Organic Molecules*, Academic Press Inc.: San Diego, 1991.
- (41) Schofield, W. C. E.; McGettrick, J.; Bradley, T. J.; Badyal, J. P. S.; Przyborski, S. Rewritable DNA Microarrays. *J. Am. Chem. Soc.* **2006**, *128*, 2280–2285.
- (42) Kade, M. J.; Burke, D. J.; Hawker, C. J. The Power of Thiol-Ene Chemistry. *J. Polym. Sci., Part A: Polym. Chem.* **2010**, *48*, 743-750.
- (43) Ladet, S.; Gravanga, P. Functionalized Adhesive Medical Gel. *Patent* WO2010095048, August 26, 2010.
- (44) Oswald, A. A.; Griesbaum, K. Radical Additions of Thiols to Diolefins and Acetylenes. In *The Chemistry of Organic Sulfur Compounds*. Kharasch, N.; Meyers, C. Y. Eds.; Pergamon Press: Oxford; 1966, Vol. 2; p 243.
- (45) Cole, M. A.; Jankousky, K. C.; Bowman, C. N. Redox Initiation of Bulk Thiol-Ene Polymerizations. *Polym. Chem.* **2013**, *4*, 1167–1175.
- (46) Nguyen, K. D. Q.; Megone, W. V.; Kong, D.; Gautrot, J. Thiol-Ene Cross-Linking and Functionalisation of Polydimethylsiloxane for Biomedical Applications *Front. Bioeng. Biotechnol.* Conference, 10th World Biomaterials Congress, Montreal, Canada, May 17–22, 2016.
- (47) Stringley, N. H. Highly Resilient Polybutadiene Ball. *Patent* US3241834, March 22, 1966.
- (48) Kato, H.; Nakatsubo, F.; Abe, K.; Yano, H. Crosslinking via Sulfur Vulcanization of Natural Rubber and Cellulose Nanofibers Incorporating Unsaturated Fatty Acids. *RSC Adv.* **2015**, *5*, 29814– 29819.
- (49) Hiraoka, H.; Kitaoh, K.; Maruoka, K.; Yamada, M. One-Piece Solid Golf Ball. *Patent* US4974852, December 4, 1990.
- (50) Kloxin, C. J.; Scott, T. F.; Bowman, C. N. Stress Relaxation via Addition-Fragmentation Chain Transfer in a Thiol-Ene Photopolymerization. *Macromolecules* **2009**, *42*, 2551–2556.
- (51) Matonis, V. A. Contemporary Thermoplastic Materials. In *Polymer Handbook*, 2nd ed.; Brandrup, J.; Immergut, E. H. Eds.; Wiley: New York, 1975; p VIII-6.

- (52) *Handbook of Modern Packaging Industries*, 2nd ed.; Asia Pacific Business Press Inc.: New Delhi, 2010; p 725–726.
- (53) Massey, L. K. *Permeability Properties of Plastics and Elastomers: A Guide to Packaging and Barrier materials*, 2nd ed.; Plastics Design Library, Norwich, 2003; p 456.
- (54) McKeen, L. W. *Permeability Properties of Plastics and Elastomers*, 3rd ed.; Elsevier Inc.: Waltham, 2012; p14.
- (55) Brummelhuis, N. T.; Diehl, C.; Schlaad, H. Thiol-Ene Modification of 1,2-Polybutadiene using UV Light or Sunlight. *Macromolecules* **2008**, *41*, 9946–9947.
- (56) Justynska, J.; Hordyjewicz, Z.; Schlaad, H. Toward a Toolbox of Functional Block Copolymers via Free-Radical Addition of Mercaptans. *Polymer* **2005**, *46*, 12057–12064.
- (57) Wang, G.; Fan, X.; Huang, J. Investigation of Thiol-Ene Addition Reaction on Poly(isoprene) under UV Irradiation: Synthesis of Graft Copolymers with “V”-Shaped Side Chains. *J. Polym. Sci., Part A: Polym. Chem.* **2010**, *48*, 3797–3806.
- (58) Kienberger, J.; Noormofidi, N.; Mühlbacher, I.; Klarholz, I.; Harms, C.; Slugovc, C. Antimicrobial Equipment of Poly(isoprene) Applying Thiol-Ene Chemistry. *J. Polym. Sci. Part A: Polym. Chem.* **2012**, *50*, 2236–2243.
- (59) Hoyle, C. E.; Lee, T. Y.; Roper, T. Thiol-enes: Chemistry of the Past with Promise for the Future. *J. Polym. Sci. Part A: Polym. Chem.* **2004**, *42*, 5301–5338.
- (60) Clayden, J.; Greeves, N.; Warren, S.; Wothers, P. *Organic Chemistry*; Oxford University Press: Oxford, 2001; p 10561–564.
- (61) Roy, S.; Gupta, B. R.; De, S. K. Epoxidised Rubbers. In *Elastomer Technology Handbook*; Cheremisinoff, N. P., Ed.; CRC Press Inc.: Boca Raton, 1993; p 640.
- (62) Lowe, A. B. Thiol-Ene “Click” Reactions and Recent Applications in Polymer and Materials Synthesis. *Polym. Chem.* **2010**, *1*, 17–36.
- (63) Decker, C.; Nguyen Thi Viet, T. Photocrosslinking of Functionalized Rubbers IX. Thiol-ene Polymerization of Styrene-Butadiene-Block-Copolymers. *Polymer*, **2000**, *41*, 3905–3912.
- (64) Apple, Inc. iPhone 6 Technical Specifications. <https://www.apple.com/iphone-6/specs/> (accessed May 17, 2016).
- (65) Samsung Electronics Ltd. Galaxy Note Edge Standard Battery Technical Specifications. <http://www.samsung.com/us/mobile/cell-phones-accessories/EB-BN915BBUSTA> (accessed May 17, 2016).

- (66) Nandivada, H.; Chen, H.-Y.; Bondarenko, L.; Lahann, J. Reactive Polymer Coatings that “Click”. *Angew. Chem. Int. Ed.* **2006**, *45*, 3360–3363.
- (67) Lowe, A. B.; Hoyle, C. E.; Bowman, C. N. Thiol-Yne Click Chemistry: A Powerful and Versatile Methodology for Materials Synthesis. *J. Mater. Chem.* **2010**, *20*, 4745–4750.
- (68) Coulson, S. R.; Woodward, I. S.; Badyal, J. P. S.; Brewer, S. A.; Willis, C. Ultra Low Surface Energy Plasma Polymer Films. *Chem. Mater.* **2000**, *12*, 2031–2038.
- (69) Ward, L. J.; Goodwin, A. J.; Merlin, P. J.; Badyal, J. P. S. Solventless Coupling of Perfluoroalkylchlorosilanes to Atmospheric Plasma Activated Polymer Surfaces *Polymer* **2005**, *46*, 3986–3991.
- (70) Sorenson, M.; Stevens, B.; Rae, A.; Chason, M. Electronic Devices with Internal Moisture-Resistant Coatings. *Patent US20150146396*, May 25, 2015.

7 TABLE OF CONTENTS ENTRY



PLASMACHEMICAL DOUBLE CLICK THIOL-ENE REACTIONS FOR WET ELECTRICAL BARRIER

(Supporting Information)

R. C. Fraser, A. Carletto, M. Wilson, and J. P. S. Badyal*

Chemistry Department, Science Laboratories, Durham University, Durham DH1 3LE,
England, UK

* Corresponding author email: j.p.badyal@durham.ac.uk

1. EXPERIMENTAL

Spin Coating of Polymer Base Layer

A 5% w/v polybutadiene solution was prepared by dissolving 2.5 g polybutadiene (Mw ~200,000, Sigma-Aldrich Co.) in toluene (99.99 wt%, Fisher Scientific Ltd.) in a 50 mL volumetric flask. The solution was agitated for 3 days (sample shaker Vibrax-VXR Model No. VX 2, IKA-Werke GmbH) to ensure that the polybutadiene had completely dissolved. Each masked micro-circuit board was fixed onto a glass plate using double sided adhesive tape (product code 1445293, Henkel Ltd.), which in turn was attached to the chuck of a spincoater (model No PRS14E, Cammax Precima Ltd.). 6 drops (~480 μ L) of the polybutadiene solution were spin coated onto the prepared micro-circuit boards at 3000 rpm and room temperature.

A 10% w/v polyisoprene solution was prepared by dissolving 2 g polyisoprene (Mw ~40,000, Sigma-Aldrich Co.) in toluene to make up to 20 mL total volume. The solution was agitated for 2 days to ensure that the polyisoprene had completely dissolved. 6 drops (~480 μ L) of the polyisoprene solution were spin coated onto the prepared micro-circuit boards at 3000 rpm and room temperature.

A 10% w/v polystyrene solution was prepared by dissolving 1 g polystyrene (Mw ~280,000, Sigma-Aldrich Co.) in toluene in a 10 ml volumetric flask. The solution was agitated for 2 days on the sample shaker to ensure that the polystyrene was completely dissolved. 3 drops (~240 μ L) of the polystyrene solution were spin coated onto the prepared micro-circuit boards at 2000 rpm and room temperature.

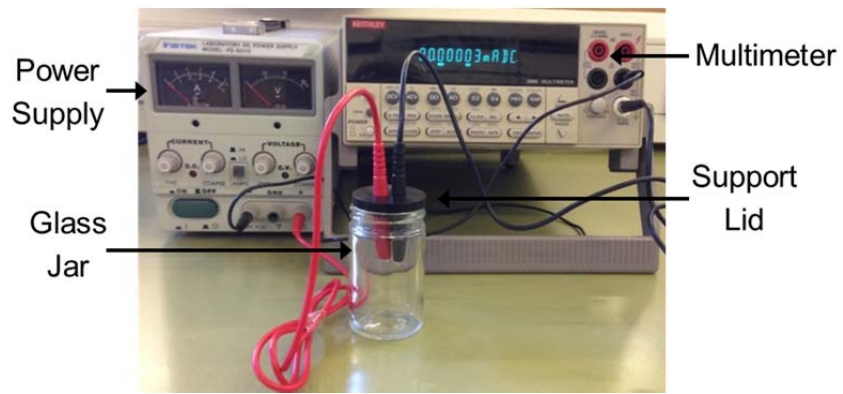


Figure S 1: Apparatus for wet electrical barrier measurement.

2. RESULTS

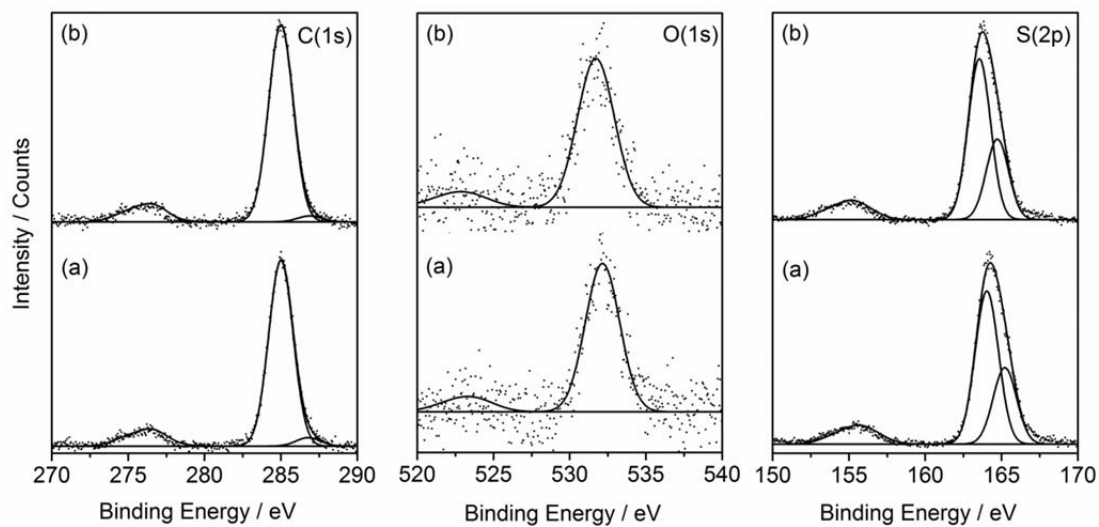


Figure S 2: High resolution XPS spectra of continuous wave 2 W plasma deposited layers: (a) 1-propanethiol; and (b) allyl mercaptan. The sulfur spectra are fitted to S(2p_{3/2}) and S(2p_{1/2}) components (separation 1.18 eV, and 2:1 relative peak area ratio).¹

Electrical Barrier Measurements

Table S 1: Wet electrical barrier measurements under an applied electric field of 10 V mm^{-1} , for a range of plasma polymers deposited onto a spin coated polybutadiene base layer (thickness $1872 \pm 39 \text{ nm}$): 1H,1H,2H,2H-perfluorooctyl acrylate (pulsed duty cycle $t_{on} = 20 \mu\text{s}$, $t_{off} = 20 \text{ ms}$, and $P_{on} = 40 \text{ W}$); glycidyl methacrylate (continuous wave 5 W); tetramethylsilane (continuous wave 3 W); and 1-propanethiol (continuous wave 2 W).

| Precursor | Plasma Polymer Thickness / nm | Log ₁₀ Electrical Barrier / $\Omega \text{ nm}^{-1}$ | |
|-------------------------------------|-------------------------------|---|-------------|
| | | t = 0 min | t = 13 min |
| 1H,1H,2H,2H-Perfluorooctyl acrylate | 299 ± 45 | 2.69 ± 1.44 | 0.64 ± 0.16 |
| | 642 ± 71 | 4.54 ± 0.64 | 2.69 ± 0.37 |
| | 984 ± 76 | † | 3.62 ± 0.07 |
| Glycidyl methacrylate | 299 ± 12 | 2.74 ± 0.06 | 1.51 ± 0.26 |
| | 574 ± 2 | 4.69 ± 0.31 | 3.39 ± 0.54 |
| | 1338 ± 59 | † | 5.25 ± 0.21 |
| Tetramethylsilane | 780 ± 38 | † | 4.87 ± 0.85 |
| | 1171 ± 20 | † | 5.03 ± 0.55 |
| 1-Propanethiol | 182 ± 11 | 2.72 ± 0.14 | 0.38 ± 0.31 |
| | 248 ± 33 | 2.89 ± 0.18 | 0.38 ± 0.21 |

† Reached the instrument detection limit of $8 \times 10^8 \Omega$.

Contact Angle Measurements

Microliter sessile drop contact angle analysis was carried out with a video capture system (VCA2500XE, AST Products Inc.) using 1.0 μL droplets of ultra-high purity water (BS 3978 grade 1).

Table S 2: Sessile water drop contact angle measurements of the plasma deposited precursors: 1H,1H,2H,2H-perfluorooctyl acrylate (pulsed duty cycle $t_{on} = 20 \mu\text{s}$, $t_{off} = 20 \text{ms}$, and $P_{on} = 40 \text{W}$); glycidyl methacrylate (continuous wave 5 W); tetramethylsilane (continuous wave 3 W); and 1-propanethiol (continuous wave 2 W). Polybutadiene and H_2S plasma treated polybutadiene (continuous wave 2 W) were control samples.

| Coating | Water Contact Angle / ° |
|--------------------------------------|-------------------------|
| Polybutadiene | 105 \pm 1 |
| 1H,1H,2H,2H-perfluorooctyl acrylate | 129 \pm 1 |
| Glycidyl methacrylate | 72 \pm 1 |
| Tetramethylsilane | 104 \pm 1 |
| 1-Propanethiol | 85 \pm 1 |
| Allyl mercaptan | 83 \pm 2 |
| Polybutadiene / H_2S | 96 \pm 1 |

3. REFERENCES

- (1) Moulder, J. F.; Stickle, W. F.; Sobol, P. E.; Bomben, K. D. *Handbook of X-ray Photoelectron Spectroscopy*; Chastain, J., Ed.; Perkin-Elmer Corporation: Eden Prairie, 1992; pp 11–28.